Cyclic Behavior of Steel Moment-Resisting Connections Reinforced by Alternative Column Stiffener Details II. Panel Zone Behavior and Doubler Plate Detailing

DAEYONG LEE, SEAN C. COTTON, JEROME F. HAJJAR, ROBERT J. DEXTER, and YANQUN YE

After the 1994 Northridge, California, earthquake, a number of experimental and computational studies were conducted to further understand the role of panel zone shear deformation in seismic connection performance (FEMA, 2000a). Based on observations of the seismic behavior of pre-Northridge Welded Unreinforced Flange-Bolted Web (WUF-B) moment-resisting connections, and experimental and computational studies of several pre- and post-Northridge moment connection details, several conclusions regarding the effects of large panel zone shear deformation were drawn.

First, panel zone yielding is stable under large inelastic cyclic loads and is thus potentially an excellent seismic energy dissipater. Nonetheless, excessive panel zone deformation can lead to localized column flange kinking, which may increase the potential for brittle fracture and low cycle fatigue (LCF) cracking in the girder flange-to-column flange groove welds (Krawinkler, Bertero and Popov, 1971; Krawinkler, 1978; Popov, Amin, Louie and Stephen, 1986; Roeder and Foutch, 1996; El-Tawil, Vidarsson, Mikesell and Kunnath, 1999; El-Tawil, 2000; Mao, Ricles, Lu and Fisher, 2001; Roeder, 2002).

Second, large panel zone shear deformation in the connection also increases the inelastic stress and strain demands in other locations, such as the edges of the shear tab (Mao et al., 2001; Ricles, Mao, Lu and Fisher, 2002). Third, panel zone flexibility can significantly influence global stiffness and seismic response of the moment frame, and thus should be considered in frame analyses when flexible panel zones are used (for example, Charney and Johnson, 1986; Liew and Chen, 1995; Biddah and Heidebrecht, 1998; Schneider and Amidi, 1998; Biddah and Heidebrecht, 1999; Kim and Engelhardt, 2002).

As a consequence of these conclusions, the panel zone design strength and required strength included in the 1997 AISC *Seismic Provisions for Structural Steel Buildings* (AISC, 1997a), hereafter referred to as the AISC Seismic Provisions, were modified in two supplements (AISC, 1999a, 2000) to provide a panel zone strength and stiffness level sufficient to prevent excessive panel zone deformation. The AISC (2000) provisions were retained, largely unchanged, in the 2002 AISC Seismic Provisions (AISC, 2002). A stiffer panel zone forces most of the yielding in the connection region into the girder and thus causes a plastic hinge to form in the girder if the Strong Column-Weak Beam (SCWB) criteria (AISC, 2002) are satisfied.

Many specimens tested after the Northridge earthquake and satisfying the requirements of FEMA (2000a) and AISC (2002) have shown good cyclic performance and higher ductility using a wide range of panel zone strengths. The few recently tested specimens that have had weak (in other words, underdesigned) panel zones have also performed satisfactorily (for example, Bjorhovde, Goland and Benac, 1999; Choi, Stojadinovic and Goel, 2000; Wongkaew, Goel and Stojadinovic, 2001; Jones, Fry and Engelhardt, 2002; Lee, Cotton, Dexter, Hajjar, Ye and Ojard, 2002). The panel zone deformations of these specimens were much larger than $4\gamma_y$ (where γ_y is panel zone shear yield strain), which was assumed by Krawinkler (1978) as the panel zone shear deformation at which the ultimate shear strength of the panel zone was developed in a joint. Nevertheless, those specimens completed the SAC loading history (SAC, 1997) up to the 4.0% interstory drift cycles without significant strength degradation.

This paper reports on research on the panel zone behavior of the Welded Unreinforced Flange-Welded Web (WUF-W) moment-resisting connection, which is outlined

Daeyong Lee is research engineer, RIST Steel Structure Research Laboratory, Hwaseong, Kyeonggi-Do, Republic of Korea.

Sean C. Cotton is structural engineer, Hammel Green and Abrahamson, Inc., Minneapolis, MN.

Jerome F. Hajjar is professor, department of civil and environmental engineering, University of Illinois, Urbana, IL.

Robert J. Dexter is associate professor (deceased), department of civil engineering, University of Minnesota, Minneapolis, MN.

Yanqun Ye is structural engineer, Thornton-Tomasetti Engineers, Chicago, IL.

in detail in (FEMA, 2000a). The objectives of this research were to reassess nonseismic and seismic design provisions for column reinforcement and to explore alternative column stiffening details that avoid welding in the column *k*-area (AISC, 1997b; Tide, 2000). As part of this research, acceptable minimum seismic panel zone design criteria were reassessed for this connection and related steel moment-resisting connections.

For this work, a total of nine pull-plate specimens were tested monotonically (Prochnow, Dexter, Hajjar, Ye and Cotton, 2000; Hajjar, Dexter, Ojard, Ye and Cotton, 2003), six full-scale WUF-W cruciform specimens were tested cyclically (Lee et al., 2002), and corroborating three-dimensional nonlinear finite element analysis was conducted (Ye, Hajjar, Dexter, Prochnow and Cotton, 2000). A companion paper (Lee, Cotton, Hajjar, Dexter and Ye, 2005) summarizes the results of the cruciform specimens. It was originally planned to test five WUF-W specimens, but one additional cruciform specimen (Specimen CR4R) was fabricated and tested due to premature brittle failure of the girder flange-to-column flange groove welds in one of the initial five specimens [Specimen CR4—the brittle failure of this specimen was not related to the panel zone behavior and is discussed in Lee et al. (2002, 2005)].

These cyclic tests were designed primarily to allow for investigation of the AISC Local Flange Bending (LFB) (AISC, 1999b), Local Web Yielding (LWY) (AISC, 1999b), and Panel Zone (PZ) (AISC, 1999b, 2002) design criteria for seismic applications. Relatively weak panel zones were designed for the WUF-W cruciform specimens with the intent of causing large localized strain concentrations in the column elements, girder elements, and connecting welds, and of exceeding the panel zone shear deformation of the $4\gamma_y$. These conditions were thus intended to increase the potential for brittle fracture and low cycle fatigue (in other words, to simulate a possible "worst-case" connection configuration) so as to evaluate the alternative column reinforcement details. The evaluation of the current AISC LFB and LWY design criteria are covered in the companion paper (Lee et al., 2005) and in Hajjar et al. (2003).

This paper presents a study of the cyclic panel zone behavior of the WUF-W cruciform specimens and an assessment of the AISC seismic panel zone design criteria for these connections. In addition, two possible modifications for seismic panel zone design criteria are proposed, including one that provides a more accurate assessment of panel zone nominal strength for steel moment-resisting connections, and a panel zone shear required strength equation that targets permitting up to $8\gamma_y$ panel zone shear deformation for WUF-W and similar connections.

RECENT CHANGES IN AISC SEISMIC PANEL ZONE DESIGN PROVISIONS

AISC (1999b) and AISC (2002) include the following panel zone shear design strength (or capacity) equation that is used for the majority of panel zone designs:

$$\phi_v R_v = \phi_v 0.6 F_{yc} d_c t_p \left(1 + \frac{3 b_{cf} t_{cf}^2}{d_g d_c t_p}\right) \tag{1a}$$

where

ϕ_v = resistance factor
R_v = nominal panel zone shear strength
F_{yc} = column minimum specified yield stress
b_{cf} = column flange width
t_{cf} = column flange thickness
d_c = column depth
d_g = girder depth
t_p = panel zone thickness

Other than changes in the resistance factor, ϕ_v, and minor changes in some of the coefficients, this equation has changed little in several editions of the specification, and is originally based on research by Krawinkler et al. (1971) and Krawinkler (1978). In addition, AISC (2002) contains the following additional provision for Special Moment Frames (SMF):

$$t \geq \left(d_z + w_z\right) / 90 \tag{1b}$$

where

t = column web or doubler plate thickness; or total thickness if doublers are plug welded
d_z = panel zone depth
w_z = panel zone width

Lee et al. (2002) provide detailed background on both of these equations.

While the nominal panel zone shear strength, R_v, has changed little for seismic design, both the required panel zone shear strength, R_u, and the resistance factor, ϕ_v, associated with R_v have been evolving. During the last 15 years, the AISC seismic panel zone required strength, R_u, has been based either on the use of load combinations or on calculation of the plastic flexural strength of the connected girders (AISC, 1992, 1997a, 1999a, 1999c, 2000, 2002). In AISC (2000, 2002), the required strength, R_u, was modified to account for the expected material overstrength and strain-hardening effects on the performance of steel moment-resisting connections, and due to the change of girder plastic hinge location from the girder-to-column interface to an appropriate distance along the girder length away from the column face, depending on the type of connection (FEMA, 2000a). AISC (2000, 2002) also increased the resistance factor, ϕ_v, from 0.75 to 1.0 for seismic design for reasons discussed later.

Table 1. Test Matrix of Cruciform Specimens					
	CR1	CR2	CR3	CR4 and CR4R	CR5
Girder	W24×94	W24×94	W24×94	W24×94	W24×94
Column	W14×283	W14×193	W14×176	W14×176	W14×145
Doubler Plate (DP)	None	Detail II	Detail II	Detail III Box (Offset)	Detail I
DP Thickness	NA	0.625 in.	2 @ 0.5 in.	2 @ 0.75 in.	2 @ 0.625 in.
Continuity Plate (CP)	None	None	Fillet-welded	None	None
CP Thickness	NA	NA	0.5 in.	NA	NA

The major changes in the AISC Seismic Provisions for the required panel zone shear strength, R_u, and the resistance factor, ϕ_v, are summarized next.

1992 AISC Seismic Provisions (AISC, 1992)

In AISC (1992), R_u was determined from elastic analyses due to load combination equations listed in the provisions. However, R_u was permitted to be capped by the shear forces determined from $0.9\Sigma\phi_b M_p$, where ϕ_b is equal to 0.9 and M_p is the girder plastic moment, $Z_g F_{yg}$ (where Z_g and F_{yg} are the plastic section modulus and specified minimum yield stress of the girder, respectively). These applicable load combinations, along with a resistance factor for panel zone shear strength of $\phi_v = 0.75$, were intended to give roughly the same level of reliability as compared with UBC (1991).

1997 AISC Seismic Provisions (AISC, 1997a)

In AISC (1997a), R_u was determined from load combination equations listed in the provisions, but was permitted to be capped by the shear due to $0.8\Sigma R_y M_p$, where $R_y M_p$ is the expected plastic moment based on an assumed increase in yield strength in the girder beyond the specified minimum value, reflected through the value of R_y. The load combination equations were similar to the load combination equations from AISC (1992), except that an amplification of the earthquake forces by the structural overstrength factor, Ω_o, was added, and the earthquake loads were taken as specified in ASCE (1995). These provisions, however, were still intended to provide the same reliability as UBC (1991).

1997 AISC Seismic Provisions — Supplement No. 1 (AISC, 1999a)

In Supplement No. 1 (AISC, 1999a), R_u was determined from the same load combination equations as AISC (1997a), but were permitted to be capped by the shear due to $0.8\Sigma M^*_{pb}$, where $\Sigma M^*_{pb} = \Sigma(1.1 R_y M_p + M_v)$, and M_v is the additional moment due to projecting the expected moments at the plastic hinge locations to the column faces. The change from $R_y M_p$ to M^*_{pb} in the moment summation was made to be consistent with the definition of the girder moment strength used for the SCWB criteria check in AISC (1997a).

1997 AISC Seismic Provisions — Supplement No. 2 (AISC, 2000)

The use of the load combination equations from AISC (1997a) was no longer permitted, as it was recognized these combinations do not directly relate to achieving yielding of the girders. Rather, the provisions state that the thickness of the panel zone must be based on the method used to proportion tested (or prequalified) connections. However, as a minimum, R_u should be determined from the summation of the moments at the column faces as determined by projecting the expected moments at the plastic hinge locations to the column faces. One major change from the previous supplement was the removal of the factor of 0.8 from the girder moments. A second major change in this supplement was an increase in the resistance factor, ϕ_v, from 0.75 to 1.0 to facilitate a direct comparison between column panel zone yielding and girder yielding. These two changes should also be applied to the recommendations of AISC (1999c), which was originally based on AISC (1997a).

2002 AISC Seismic Provisions (AISC, 2002)

The 2002 AISC Seismic Provisions (AISC, 2002) retained the design provisions for panel zone required strength, panel zone design strength, and the strong-column weak-beam design of AISC (2000).

CRUCIFORM TEST SPECIMENS

Table 1 shows the matrix of specimens tested in this research. Cruciform specimens were used in which two girders framed into a column (pinned at both ends) using the WUF-W connection (Figure 1a shows typical fabrication details). Antisymmetric loads were then applied to the girder

tips. All rolled sections were fabricated from ASTM A992 wide-flange sections, and ASTM A572 Grade 50 steel was selected for all stiffener materials. Details of the testing configuration, specimen, measured material properties, loading protocols, and connection performance are given in Lee et al. (2002, 2005).

Three doubler details were tested in this experimental study (see Figure 1b). Doubler plate Detail I and Detail II represent two different fillet-welded details, while doubler plate Detail III represents a groove-welded box (offset) detail. Specimen CR4R features the box (offset) doubler plate detail, and it was expected that this type of detail would be less than fully effective, based on the results of Bertero, Krawinkler and Popov (1973). Thus, the doubler plates in that specimen were approximately 30% thicker than those of Specimen CR3, which has the same W24×94 girder section and W14×176 column section. All doubler plates were extended vertically 6 in. above and below the girder flanges (see Figure 1a).

One continuity plate detail was also tested, in which the plate thickness was approximately equal to half the girder flange thickness, and the plate was fillet-welded to both the column flanges and doubler plates. The size of the fillet welds needed for both doubler and continuity plate details were calculated using procedures given in AISC (1999c). One completely unstiffened specimen with a W14×283 column (Specimen CR1) was also tested to verify the cyclic response of a specimen without continuity plates and doubler plates. In addition, Specimens CR2 and CR5 had no continuity plates although continuity plates were required as per AISC (1992) for Specimen CR2 and as per AISC (1992, 1999b, 1999c) for Specimen CR5 (Lee et al., 2002, 2005). These specimens were used to examine the response of a column flange subjected to the LFB limit state under cyclic loading.

To investigate the effects of recent AISC seismic design criteria changes on member selection and panel zone design in a joint, the nominal beam-to-column moment ratios and panel zone design capacity/demand ratios for the five successfully tested WUF-W cruciform specimens are calculated and compared in Table 2. It is clear that the 1997 AISC Seismic Provisions (AISC, 1997a) and later provisions require much stronger column members due to the revised SCWB provisions (not detailed here for brevity) as compared with the 1992 AISC Seismic Provisions (AISC, 1992). This is because the calculated girder moment, as per AISC (1992), is approximately 1.4 times smaller for the same girder section as compared with AISC (1997a) and later provisions, since the probable girder plastic moment and the additional moment increase due to shear amplification are considered in these later specifications. As shown in Table 2, only Specimens CR1 and CR2 (strictly speaking, Specimen CR1 only) satisfied the SCWB criteria for AISC (1997a) or later. However, all specimens satisfy the SCWB criteria of AISC (1992).

For the calculation of the panel zone shear required strength in Table 2, the defined maximum or minimum panel zone required strengths in each of the AISC seismic provisions are used instead of any load combinations. The results in Table 2 indicate that AISC (2000) and AISC (2002) require somewhat stronger panel zones as compared with (AISC, 1997a). The panel zones designed by AISC (2000) and AISC (2002) are moderately stronger when compared with the panel zones designed by AISC (1992). Only Specimen CR4R satisfies the panel zone design criteria of both AISC (1992) and AISC (1997a). The panel zone of Specimen CR4R, however, is slightly underdesigned as per AISC (2000) and AISC (2002), in other words, $\phi_v R_v / R_u = 0.93$. Under AISC (2002), the nominal panel zone design capacity/demand ratios of the other four WUF-W specimens are approximately 0.7 (in other words, $\phi_v R_v / R_u \approx 0.7$).

CYCLIC PANEL ZONE BEHAVIOR

This section summarizes the cyclic panel zone behavior of the five WUF-W cruciform specimens discussed in conjunction with Tables 1 and 2. The experimental results are

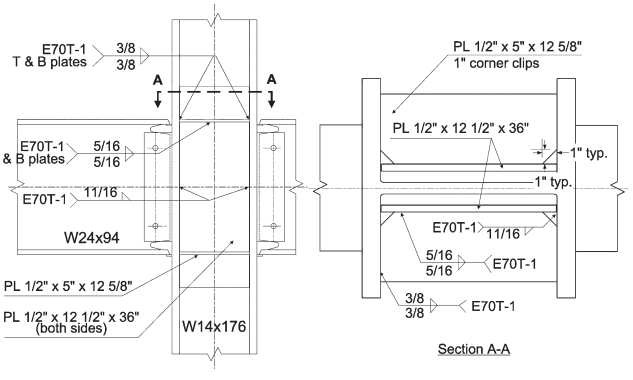

Fig. 1a. Typical welding details used for cruciform specimens (Specimen CR3).

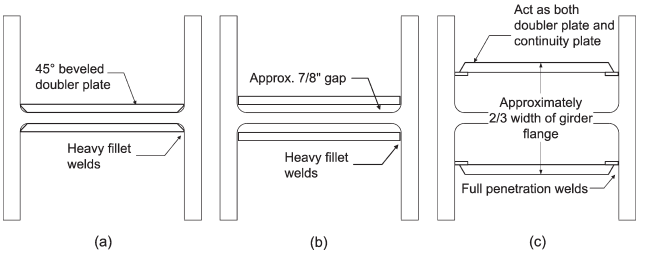

Fig. 1b. Doubler details: (a) back-beveled fillet-welded doubler (Detail I), (b) square-cut fillet-welded doubler (Detail II), (c) box (offset) doubler (Detail III).

Table 2. Comparison of Nominal Beam-to-Column Moment Ratios (SCWB Criterion) and Panel Zone Design Capacity/Demand Ratios, $\phi R_v/R_u$					
	CR1	CR2	CR3	CR4R	CR5
Column-Beam Moment Ratio (SCWB Criterion)					
1992 Seismic Provisions (AISC, 1992)	2.13	1.40	1.26	1.26	1.02
1997 Seismic Provisions (AISC, 1997a)	1.50	0.99	0.89	0.89	0.73
2002 Seismic Provisions (AISC, 2002)	1.50	0.99	0.89	0.89	0.73
Panel Zone Design Capacity/Demand Ratio ($\phi R_v/R_u$)					
1992 Seismic Provisions (AISC, 1992)	0.89	0.81	0.92	1.14	0.91
1997 Seismic Provisions (AISC, 1997a)	0.82	0.75	0.85	1.05	0.84
1997 Seismic Provisions Supplement No.2 (AISC, 2000)	0.72	0.66	0.74	0.93	0.74
2002 Seismic Provisions (AISC, 2002)	0.72	0.66	0.74	0.93	0.74
2002 Seismic Provisions (AISC, 2002) with demand computed from Equation (14)	0.85	0.78	0.87	1.09	0.87
Strength computed from Equation (13) with demand computed from Equation (14)	0.65	0.64	0.74	0.93	0.75

compared with the panel zone strengths predicted by the 2002 AISC seismic panel zone equation presented in Equation 1a, with a focus on the effects of the larger panel zone shear deformation on the cyclic performance of the WUF-W moment connection.

The SAC (1997) loading history was used for all experiments. Specimens CR1, CR2, CR3, CR4R and CR5 completed the SAC (1997) loading history up to two cycles at 4.0% interstory drift without significant strength degradation (Lee et al., 2002, 2005). Additional cycles at the same drift level were applied until the specimen failed or until the specimen showed a significant degradation in its strength. Each specimen was subjected to a total of 14 (CR1), 16 (CR2), 14 (CR3), 12 (CR4R) and 6 (CR5) 4.0% interstory drift cycles, respectively, before a noticeable strength drop due to low cycle fatigue fracturing in the girder flange-to-column flange groove welds was observed. In all of these specimens, initial local yielding was observed in girder flanges at an early stage of the loading history, in other words, the 0.5% to 0.75% interstory drift level. Widespread panel zone yielding was first visible during the 1.0% (in the column web of CR1), 1.0% (in the column web of CR2), 1.5% (in the doubler plate of CR2), 1.5% (in the doubler plate of CR3), 2.0% (in the doubler plate of CR4R), and 2.0% (in the doubler plate of CR5) interstory drift cycles, respectively. The panel zones fully yielded during the 3.0% interstory drift cycles in Specimens CR1, CR2 and CR3, and during the 4.0% interstory drift cycles in Specimens CR4R and CR5. Details of the results of these tests are presented in Lee et al. (2002, 2005).

To investigate the global cyclic response of the WUF-W cruciform specimens, the total plastic rotation and the components of plastic rotation within the connection elements are compared in Table 3. In Table 3, the total plastic rotation relative to the column centerline was determined by subtracting the measured elastic rotation relative to the column centerline from the total rotation relative to the column centerline, calculated from the vertical displacement at the tip of each actuator divided by the distance from the actuator to the column centerline. For the determination of the elastic stiffness, the values of the girder tip load and vertical displacement at the first peak of 0.375% interstory drift were used. Similarly, the girder plastic rotation relative to the column face was determined by subtracting the measured girder elastic rotation relative to the column face from the total girder rotation relative to the column face measured at the assumed plastic hinge location [see Figure 2a for the associated placement of the linear variable differential transducers (LVDTs)]. This girder plastic rotation relative to the column

Table 3. Decomposition of Total Plastic Rotation in Cruciform Specimens

	CR1		CR2		CR3		CR4R		CR5	
	East	West	East	West	East	West	East	West	East	West
Maximum Interstory Drift (Radian x 100)	4.00	4.00	4.00	4.00	4.00	4.00	4.00	4.00	4.00	4.00
Total Plastic Rotation Relative to Column Centerline (Radian x 100)	2.50	2.54	2.41	2.40	2.26	2.23	2.13	2.15	2.13	2.16
Girder Plastic Rotation Relative to Column Centerline (Radian x 100)	0.79	0.72	1.01	0.97	0.98	0.91	1.05	0.93	0.97	0.93
Panel Zone Plastic Rotation (Radian x 100)	2.04		1.90		1.94		1.07		1.45	
Column Plastic Rotation (Radian x 100)	Negligible[a]									

[a] Specimen CR5 exhibited yielding in the column just above and below the girder depth, but the column plastic rotation was not measured.

face was converted to the girder plastic rotation relative to the column centerline using the following equation:

$$\theta_{p,g}^{CL} = \theta_{p,g}\left(\frac{L_g}{L_g + d_c/2}\right) \quad (2)$$

where

$\theta_{p,g}^{CL}$ = girder plastic rotation relative to column centerline

$\theta_{p,g}$ = girder plastic rotation relative to the column face

L_g = girder length between loading point and column face

The panel zone plastic shear deformation was determined by subtracting the measured panel zone elastic shear deformation from the total panel zone shear deformation, which was calculated from two LVDTs placed in the panel zone, as shown in Figures 2a and 2b. Referring to Figure 2b, the total panel zone shear deformation was given as

$$\gamma_{pz} = \frac{|\Delta_1| + |\Delta_2|}{2}\frac{\sqrt{b'^2 + h'^2}}{b'\,h'} \quad (3)$$

where

γ_{pz} = average total panel zone shear deformation

Δ_1, Δ_2 = displacements of two diagonal LVDTs

b' = width of panel zone between two LVDT anchor points

h' = height of panel zone between two LVDT anchor points

The panel zone plastic rotation is calculated from the panel zone plastic shear deformation, using the following expression from Leon (1983):

$$\theta_{p,pz}^{CL} = \frac{1}{\left(L_g + d_c/2\right)}\left[\frac{\gamma_{p,pz}L_g\left(L_c - d_g\right)}{L_c} - \frac{\gamma_{p,pz}d_g d_c}{2L_c}\right] \quad (4)$$

where

$\theta_{p,pz}^{CL}$ = panel zone plastic rotation

$\gamma_{p,pz}$ = panel zone plastic shear deformation

L_c = column length between pin centerlines

In this experimental study, the column plastic rotation was not measured because this portion is typically very small and usually negligible once the SCWB criteria are met in the connection. As shown in Table 2, all specimens satisfied the SCWB criteria of the 1992 AISC Seismic Provisions (AISC, 1992), while the column-to-girder moment ratios of the specimens, except for Specimen CR5, satisfied or were close to the limit of the SCWB criteria from AISC (2000, 2002). The results presented in Table 3 indicate that most of the plastic rotation occurred in the panel zones (rather than through girder plastification) in Specimens CR1, CR2, CR3 and CR5 during the 4.0% interstory drift cycles. Specimen CR4R, because of its larger doubler plates, showed an approximately equal proportion of plastic rotation between the girder and the panel zone during the 4.0% interstory drift cycles.

In spite of the different column stiffener details and different strength ratios among the connection elements, Specimens CR1, CR2, and CR3 showed comparable cyclic panel zone response. In particular, the pattern and amount of panel zone yielding at each drift level was very similar for each of those three specimens. These experimental results will be further discussed later in this paper in comparison with the panel zone strengths predicted by Equation 1a. Specimen CR4R showed the smallest amount of the panel zone yielding up to the 4.0% interstory drift cycles, for reasons discussed earlier. In contrast, the column flanges of Specimen CR5 significantly yielded just above and below the girder flanges during the 4.0% interstory drift cycles. At this drift level, a major portion of yielding in the column of Specimen CR5 seemed to be redistributed between the column flanges and panel zone.

Yielding in the five specimens during the 4.0% interstory drift cycles are presented in Figure 3. In all specimens, the girder plastic moment strength was achieved by the 4.0% interstory drift cycles. However, only minor girder web yielding was observed in most of these specimens just before the low cycle fatigue rupturing occurred in the girder flange-to-column flange groove welds (Lee et al., 2002, 2005). In addition, with these weaker panel zones, as shown in Figure 3, major girder yielding occurred near the girder flange-to-column flange junction area instead of in the plastic hinge location that is assumed in most of the moment-resisting connections discussed in FEMA (2000a) (in other words, $d_g/2$ location away from the column face). Even in Specimens CR1 and CR2, which satisfied the SCWB criteria of AISC (2002), a major portion of the girder yielding was observed in the flanges near the junction area. This observation indicates that it may be more realistic to calculate the panel zone shear required strength directly at the column face for the WUF-W connection in the case of columns with weaker panel zones, without considering the increment in the moment due to the girder shear force at the assumed plastic hinge location, for example, a distance of $d_g/2$ away from the column face, as would be typically calculated in AISC (2002).

PANEL ZONE NOMINAL STRENGTH BASED ON $4\gamma_y$

The use of weak panel zones in these test specimens ensured that all panel zones exceeded the shear deformation of $4\gamma_y$ implied by the AISC panel zone equation expressed in Equation 1a (a limiting shear deformation of $4\gamma_y$ is approximately

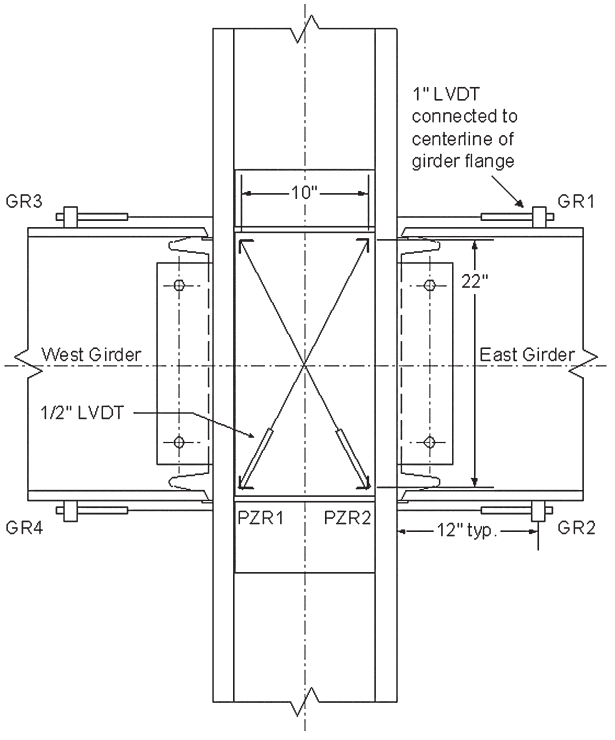

Fig. 2a. Girder and panel zone LVDT placement for all specimens.

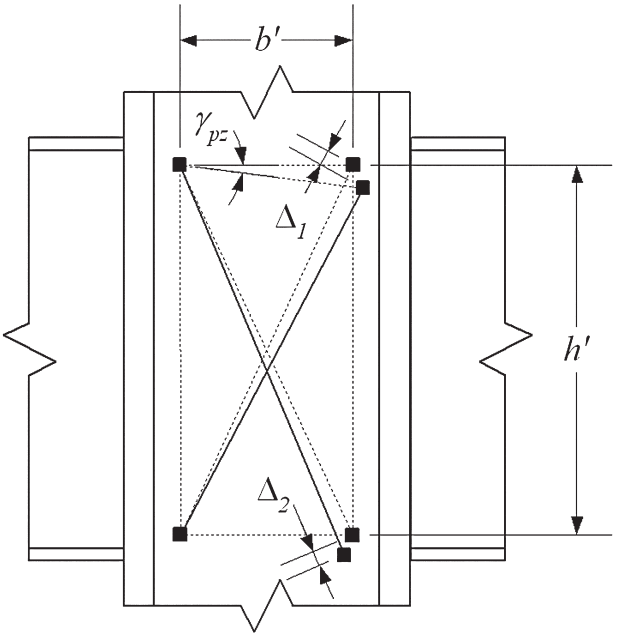

Fig. 2b. Panel zone shear deformation measurement.

(a) CR1

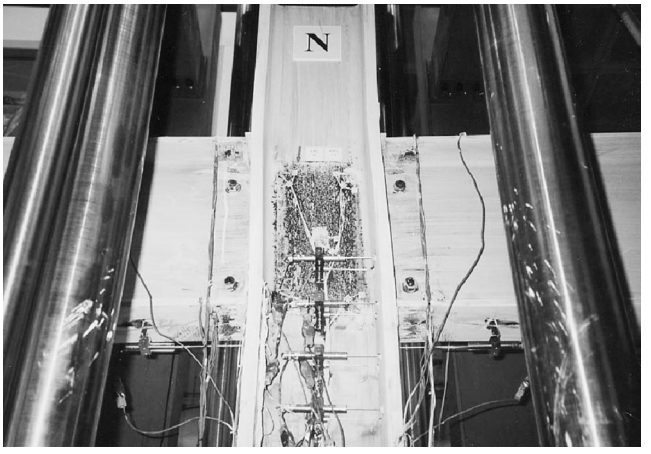

(b) CR2

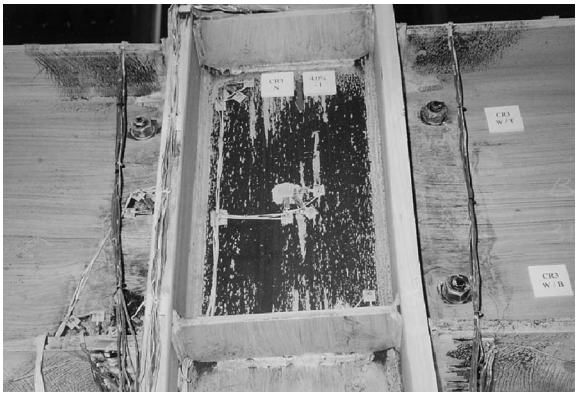

(c) CR3

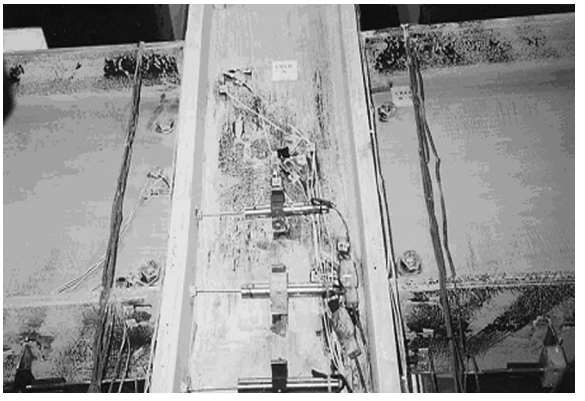

(d) CR4R

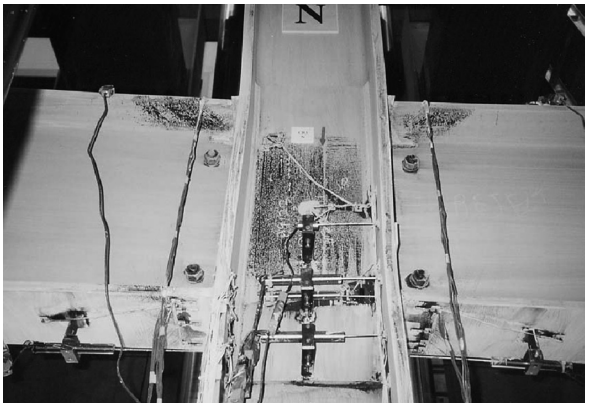

(e) CR5

Fig. 3. Yielding in the connection during a peak of the 4.0% interstory drift cycles.

implied through the derivation of that equation). In Figures 4a through 4e, the measured panel zone behavior of each specimen is compared with the panel zone strengths predicted by Equation 1a as per AISC (2002). In these figures, the total panel zone shear deformations are calculated by using Equation 3, and the experimental panel zone shear forces are calculated through the following relations:

$$V_{pz} = \frac{M_{tot}}{d_g} - V_c \tag{5}$$

where

V_{pz} = experimental panel zone shear force
M_{tot} = total moment at the column face = $P_{tot}L_g$
P_{tot} = sum of absolute values of East and West actuator loads
V_c = shear force in the column

The first term of Equation 5 is the sum of the girder flange forces delivered to the column faces, and the second term is the shear force in the column. The column shear force, V_c, is calculated from statics, resulting in the expression

$$V_c = \frac{P_{tot}\left(L_g + d_c/2\right)}{L_c} \tag{6}$$

Combining Equations 5 and 6 yields the final expression for calculating the experimental panel zone shear force:

$$V_{pz} = P_{tot}\left(\frac{L_g}{d_g} - \frac{\left(L_g + d_c/2\right)}{L_c}\right) \tag{7}$$

The first positive and negative peaks at each drift level were used to generate the experimental backbone curves in Figures 4a through 4e. In the figures, the horizontal axis is normalized by the shear yield deformation (γ_y), equal to $F_{yc}^*/\sqrt{3}G$, where G is shear modulus of elasticity (G = 11,150 ksi). The measured yield strength of the column web is used for F_{yc}^* in this calculation.

A prediction of the panel zone shear load-deformation curve may be generated from Equation 1a, using the same bilinear approximation adopted by Krawinkler (1978). The first portion of the curve is defined by the elastic stiffness, and is valid up to the point of general shear yielding of the panel zone (in other words, $V_y = 0.6F_{yc}d_ct_p$):

$$K_e = \frac{dV}{d\gamma} = d_c t_p G \qquad (0 < \gamma \le \gamma_y) \tag{8}$$

where

K_e = elastic panel zone stiffness

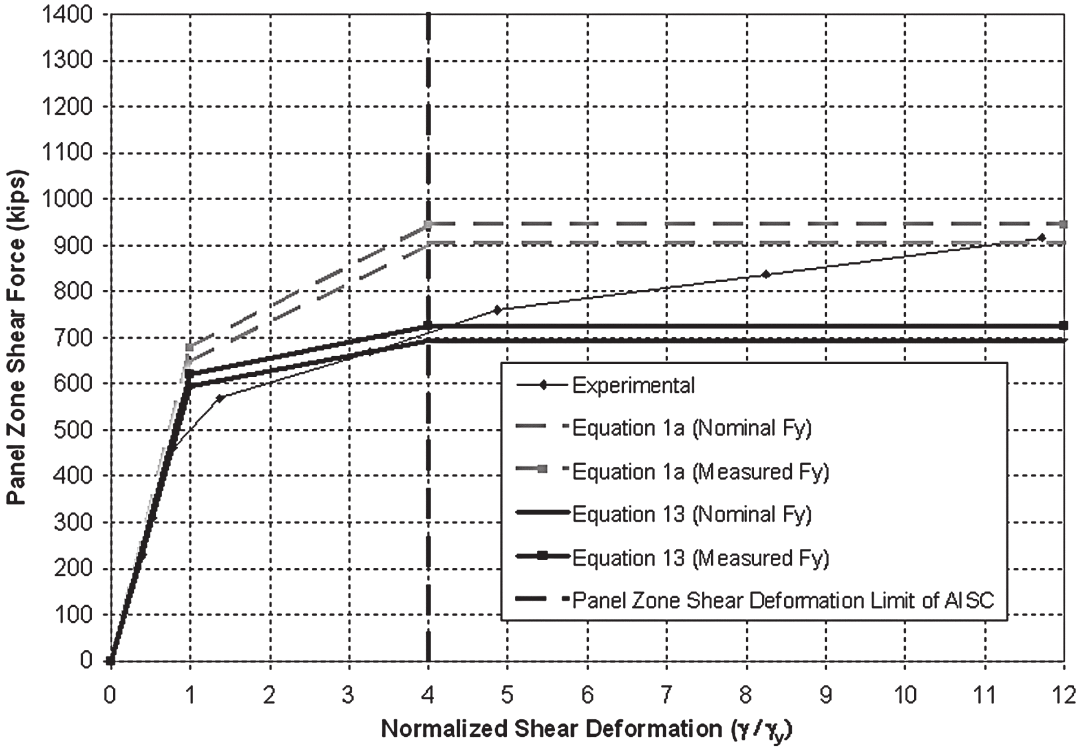

(a) CR1

Fig. 4. Backbone curve of the cyclic panel zone behavior up to the 4.0% interstory drift cycles.

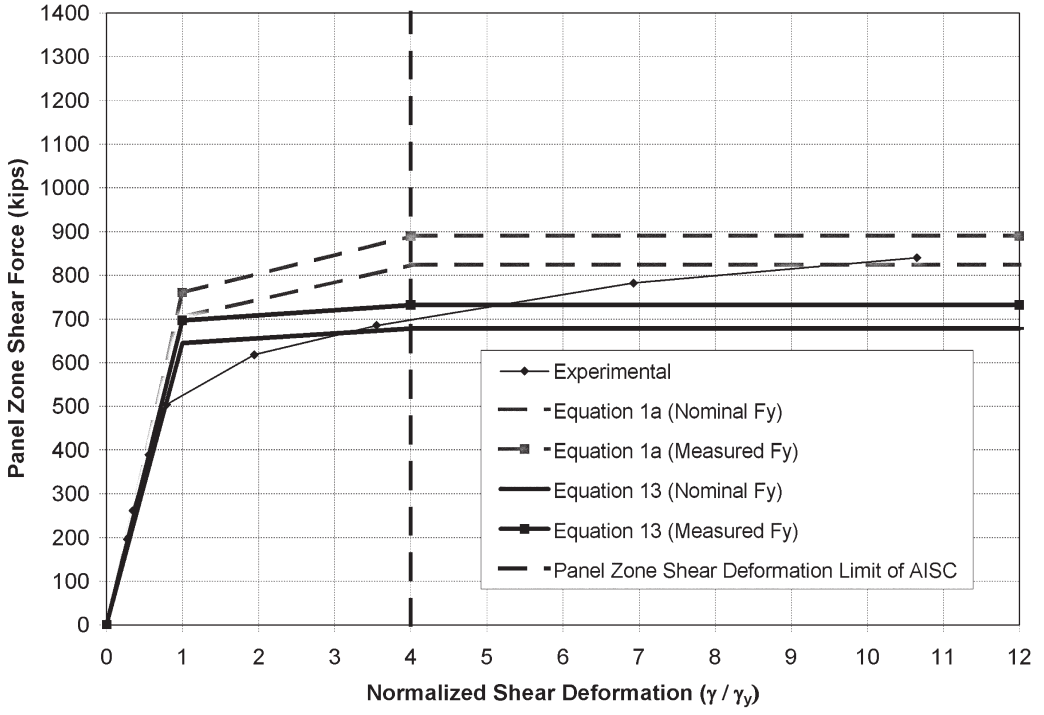

(b) CR2

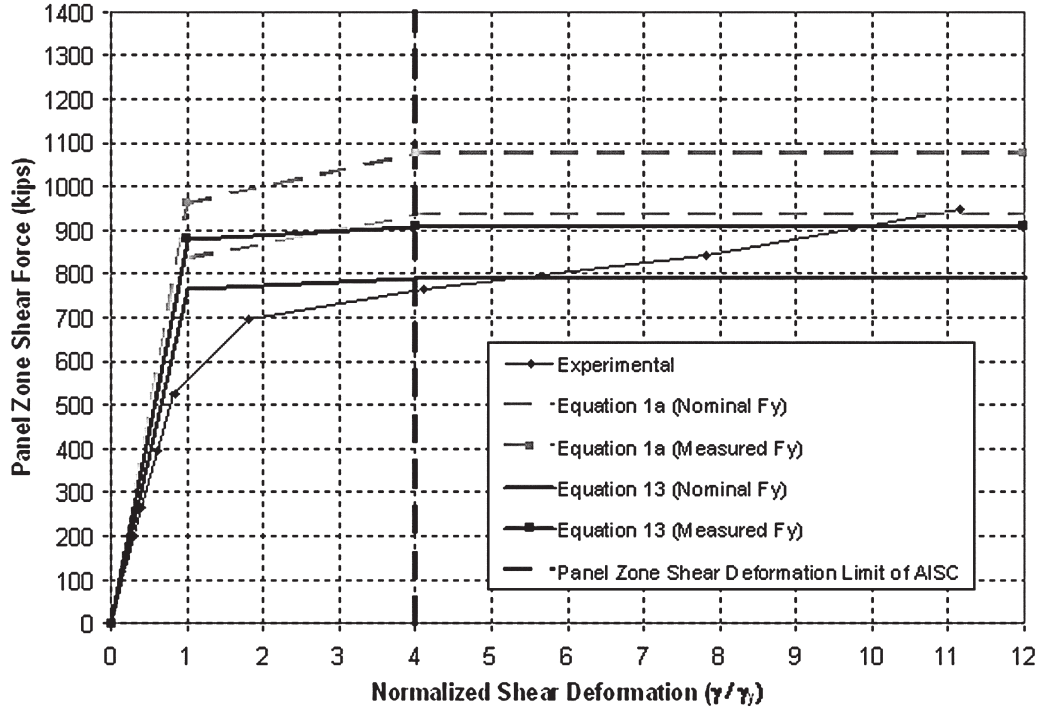

(c) CR3

Fig. 4. Backbone curve of the cyclic panel zone behavior up to the 4.0% interstory drift cycles (continued).

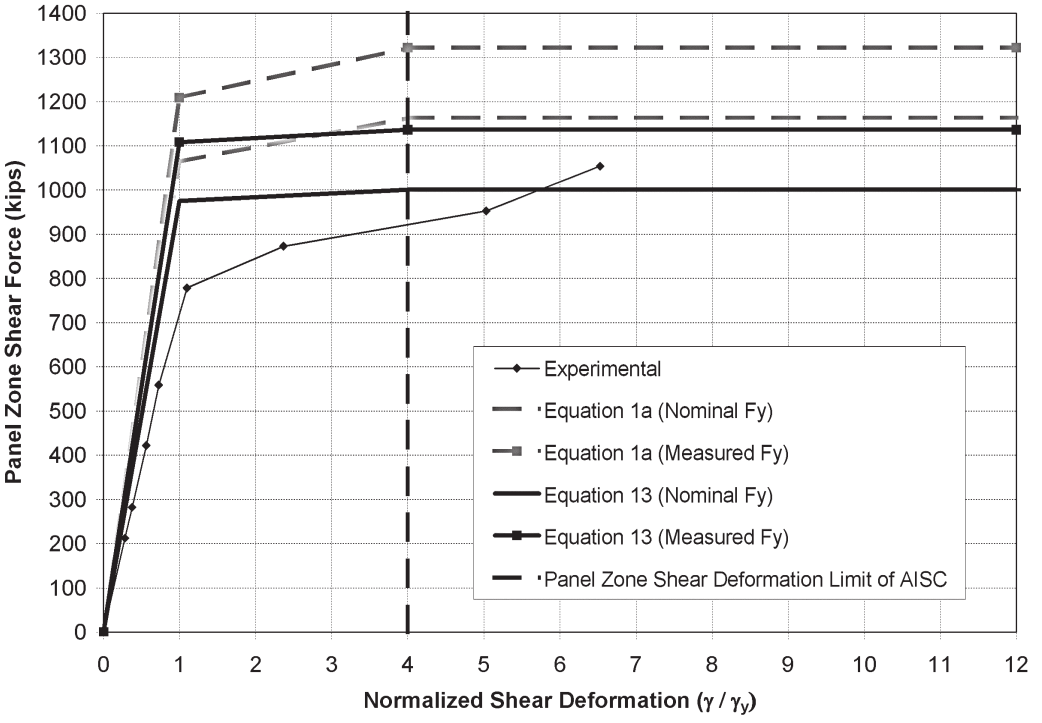

(d) CR4R

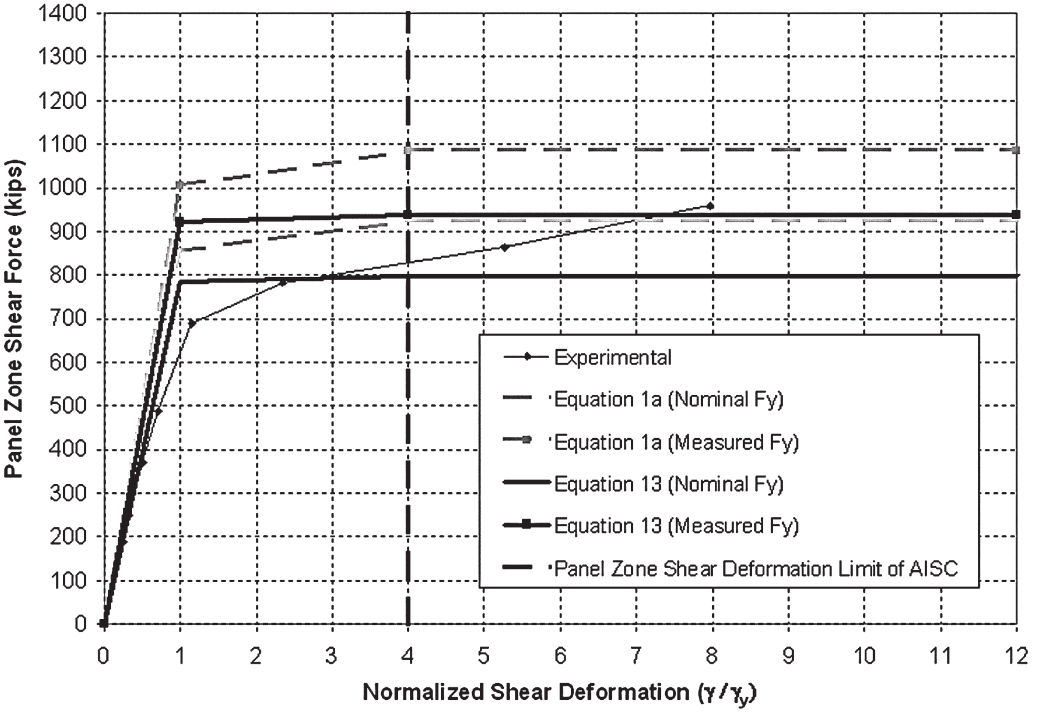

(e) CR5

Fig. 4. Backbone curve of the cyclic panel zone behavior up to the 4.0% interstory drift cycles (continued).

The second portion of the curve is defined by the post-elastic stiffness and is valid to a shear deformation of $4\gamma_y$. This deformation level was selected by Krawinkler (1978) as a limit to avoid excessive panel zone deformation. The shear force at a panel zone shear deformation of $4\gamma_y$ is that given by Equation 1a. The resulting post-elastic stiffness, K_p, is thus (Lee et al., 2002):

$$K_p = \frac{dV}{d\gamma} = \frac{b_{cf} t_{cf}^2 G}{d_g} \qquad (\gamma_y < \gamma \le 4\gamma_y) \qquad (9)$$

Potential shortcomings of the current design methodology have been discussed in other research, dating back to the original publication of the model by Krawinkler (1978). The small member sizes from the tests used to develop Equation 1a were noted, and caution was suggested when extrapolating the results to larger columns. The finite element study by El-Tawil et al. (1999) and El-Tawil (2000) indicated the present provisions overestimate the panel zone shear strength when the column flanges are very thick. The three-dimensional continuum nonlinear finite element models of the five specimens in the present research yielded predicted panel zone strengths at a deformation of $4\gamma_y$ averaging approximately 80% of the shear given by Equation 1a (Ye et al., 2000). This is consistent with the experimental results of the five specimens.

To evaluate the AISC panel zone provisions, the curves developed by Equations 8 and 9 are plotted for each specimen and compared with the experimental data in Figures 4a through 4e. Both the nominal and measured yield strengths of the column web (Lee et al., 2002, 2005) are used in the equations. The measured yield strengths of the column web are used for the panel zone strength calculations even though these values are somewhat different when compared with the measured yield strengths of the doubler plates in cases of Specimens CR2, CR3, CR4R and CR5.

It is evident from Figure 4 that the panel zone design shear strength given by Equation 1a is significantly overestimated for these specimens. For example, at $4\gamma_y$, the shear carried by the panel zone in Specimen CR1, the specimen with the thickest column flanges and a specimen which satisfies the SCWB provisions (see Table 2), was approximately 700 kips even though Equation 1a predicted 903 kips for the W14×283 column using nominal material properties. The discrepancy is more severe using the measured yield strength for the strength prediction. While the AISC (2002) nominal shear strength of 903 kips was eventually reached in this specimen, it did not occur until a deformation of over $11\gamma_y$, corresponding to the 4.0% interstory drift cycles. Similar trends are seen in the other specimens. As Equation 1a is also used for nonseismic design as per AISC (1999b), where the SCWB provisions need not be satisfied, this suggests that a reevaluation of the present design provisions for the panel zone is warranted.

Lee et al. (2002) present a revised nominal panel zone strength equation that is intended to better represent the inelastic response of panel zones, as compared with the model used to derive Equation 1a (Krawinkler et al., 1971; Krawinkler, 1978). A revision of a model for panel zone response presented by Fielding and Huang (1971) represents the panel zone as a pinned-base portal frame with a rigid girder and a shear force, V_f, applied laterally at the top of the portal frame, causing shear deformation, γ. The pinned ends represent the inflection points seen at mid-height of deformed panel zones, and the infinitely rigid girder represents the restraint imposed on the panel zone by the columns above and below the panel zone. This revised model is essentially a restatement of the Fielding and Huang (1971) model, and gives the same stiffness. Plastic hinges are assumed to form at the tops of the flange cantilevers (in other words, at the corners of the panel zone), consistent with experimental observations. The model also predicts the reverse curvature bending deformation typically exhibited by panel zones. The elastic lateral deflection of this frame representation of the panel zone is

$$\Delta = \frac{1}{2}\left(\frac{dV_f l^3}{3EI_f}\right) \qquad (10a)$$

where

Δ = lateral deflection = $l^*d\gamma$
dV_f = incremental panel zone shear force carried by column flanges
l = height of frame model = $d_g/2$
E = modulus of elasticity
I_f = moment of inertia of individual column flange

Substituting $(l^*d\gamma)$ for the deflection, Δ, $d_g/2$ for the height, l, and $b_{cf} t_{cf}^3/12$ for the column flange moment of inertia, I_f, into Equation 10a and rearranging results in the post-yield panel zone stiffness of the modified Fielding and Huang (1971) model:

$$K_p = \frac{dV_f}{d\gamma} = \frac{2Eb_{cf} t_{cf}^3}{d_g^2} \qquad (10b)$$

Assuming a maximum deformation of $4\gamma_y$, the ultimate shear strength of the panel zone can be expressed by the following [from Krawinkler (1978)]:

$$R_v = V_y\left(1 + \frac{3K_p}{K_e}\right) \qquad (11)$$

Table 4. Connection Member Sizes and Joint Type for Tests Used to Evaluate Panel Zone Nominal Strength

Test Designation	Column	Girder(s)	Connection Type	Joint Type
Fielding and Huang[1]	W14×184	W24×160	WUF-W	Exterior
Krawinkler et al.[1]: A-1	8 WF 24	10 B 15	WUF-W	Interior
Krawinkler et al.[1]: A-2	8 WF 24	10 B 15	WUF-W	Interior
Krawinkler et al.[1]: B-2	8 WF 67	14 B 22	WUF-W	Interior
Bertero et al.[1]: A-3	8 WF 24	10 B 15	WUF-W	Interior
Bertero et al.[1]: B-3	8 WF 67	12 WF 27	WUF-W	Interior
Bertero et al.[1]: B-4	8 WF 67	10 WF 29	WUF-W	Interior
Becker[1]: 1	W14×61	W14×61	WUF-W	Exterior
Becker[1]: 2	W14×61	W14×61	WUF-W	Exterior
Popov et al.[2]: 2	18" built-up	W18×40	WUF-B	Interior
Popov et al.[2]: 3	19" built-up	18" built-up	WUF-B	Interior
Popov et al.[2]: 4	19" built-up	18" built-up	WUF-B	Interior
Popov et al.[2]: 6	19" built-up	18" built-up	WUF-B	Interior
Popov et al.[2]: 7	W21×93	W18×71	WUF-B	Interior
Popov et al.[2]: 8	W21×93	W18×71	WUF-B	Interior
Ghobarah et al.: CB-1	W14×43	W14×38	Extended end plate	Exterior
Ghobarah et al.: CC-3	W12×87	W16×40	Extended end plate	Exterior
Tsai et al.: TH2	W14×159	W21×83	WUF-B	Exterior
FEMA: EERC-PN1	W14×176	W30×99	WUF-B	Exterior
FEMA: EERC-PN2	W14×176	W30×99	WUF-B	Exterior
FEMA: EERC-PN3	W14×176	W30×99	WUF-B	Exterior
FEMA: EERC-AN1	W14×176	W30×99	WUF-B + 2 cover plates	Exterior
FEMA: UCSD-1	W14×176	W30×99	WUF-B	Exterior
FEMA: UCSD-2	W14×176	W30×99	WUF-B	Exterior
FEMA: UCSD-3	W14×176	W30×99	WUF-B	Exterior
FEMA: UCB-PN1	W14×257	W36×150	WUF-B	Exterior
FEMA: UCB-RN2	W14×257	W36×150	WUF-B (repaired)	Exterior
FEMA: UCB-RN3	W14×257	W36×150	WUF-B (repaired)	Exterior
FEMA: UCB-AN1	W14×257	W36×150	WUF-B + 1 haunch	Exterior
FEMA: UTA-4	W14×257	W36×150	WUF-B + 2 cover plates	Exterior
Choi et al.: SP-9.1	W14×176	W30×99	Free-flange	Exterior
Choi et al.: SP-10.1	W14×257	W30×124	Free-flange	Exterior
Choi et al.: SP-10.2	W14×257	W30×124	Free-flange	Exterior

[1] Both the girder flanges and webs of these connections were welded to the column; these are thus identified as WUF-W connections in this table, although the connections deviated in some details from the requirements of the WUF-W connections developed for FEMA (2000a).
[2] The girder flanges of these connections were welded to the column, while the girder webs were bolted to the column through a shear tab; thus these are identified as WUF-B connections in this table, although the connections deviated in some details from the requirements of the WUF-B connections developed for FEMA (2000a).

Table 4 (continued). Connection Member Sizes and Joint Type for Tests Used to Evaluate Panel Zone Nominal Strength				
Test Designation	Column	Girder(s)	Connection Type	Joint Type
Lee et al.: SP-3.1	W14×120	W24×68	WUF-B	Exterior
Lee et al.: SP-3.2	W14×120	W24×68	WUF-B	Exterior
Lee et al.: SP-4.1	W14×145	W30×99	WUF-B	Exterior
Lee et al.: SP-4.2	W14×145	W30×99	WUF-B	Exterior
Lee et al.: SP-5.1	W14×176	W30×99	WUF-B	Exterior
Lee et al.: SP-7.2	W14×257	W36×150	WUF-B	Exterior
Ricles et al.: LU-T1	W14×311	W36×150	WUF-W	Exterior
Ricles et al.: LU-T2	W14×311	W36×150	WUF-W	Exterior
Ricles et al.: LU-T4	W14×311	W36×150	WUF-B	Exterior
Ricles et al.: LU-C1	W14×398	W36×150	WUF-W	Interior
Ricles et al.: LU-C2	W14×398	W36×150	WUF-W	Interior
U. of Minnesota: CR1	W14×283	W24×94	WUF-W	Interior
U. of Minnesota: CR2	W14×193	W24×94	WUF-W	Interior
U. of Minnesota: CR3	W14×176	W24×94	WUF-W	Interior
U. of Minnesota: CR4R	W14×176	W24×94	WUF-W	Interior
U. of Minnesota: CR5	W14×145	W24×94	WUF-W	Interior

Substituting Equations 8 and 10b into Equation 11 and replacing E with $2.6G$ yields a new ultimate strength criterion for panel zones:

$$R_v = 0.6F_{yc}d_c t_p\left(1+\frac{15.6b_{cf}t_{cf}^3}{d_g^2 d_c t_p}\right) \qquad (12)$$

At a panel zone shear deformation of $4\gamma_y$, Equation 1a predicts a post-yield strength increase above first yield ($V_y = 0.6F_{yc}d_c t_p$) of 39.4% (CR1), 17.1% (CR2), 11.9% (CR3), 9.3% (CR4R), and 8.0% (CR5), while Equation 12 predicts an increase of 17.5% (CR1), 5.3% (CR2), 3.3% (CR3), 2.6% (CR4R), and 1.9% (CR5), respectively.

Despite an improvement, Equation 12 still overpredicts the panel zone shear strength at the design deformation of $4\gamma_y$ (Lee et al., 2002). Part of the discrepancy is the assumed yield strength of the panel zone ($V_y = 0.6F_{yc}d_c t_p$); in other words, the panel zone shear force at $1\gamma_y$. The use of the 0.6 factor on shear yield strength as opposed to 0.55 results in a 9% difference between the nominal panel zone yield strengths. While the use of $0.6F_y$ can be reasonably argued for other shear applications, this appears unconservative when applied to panel zones. The use of $0.55F_y$ may be more appropriate in this case (FEMA, 2000b). The 15.6 factor in the post-yield term is also conservatively truncated to 15. The revised model is now given as

$$R_v = 0.55F_{yc}d_c t_p\left(1+\frac{15b_{cf}t_{cf}^3}{d_g^2 d_c t_p}\right) \qquad (13)$$

Figures 4a through 4e compare the experimental data to Equations 1a and 13 (no resistance factors were included, in other words, $\phi_v = 1.0$) using both the nominal and measured yield strengths of the column web. The post-yield strengths at $4\gamma_y$ are slightly underpredicted in Specimens CR1, CR2 and CR5 when the nominal yield strengths are used, but the differences are very small and negligible. For these weak panel zones, the shear strength at the onset of panel zone yielding is still overpredicted in all cases when the measured yield strengths of the column webs are used, but it is more closely approximated than using Equation 1a.

A study of past connection test data was conducted to evaluate Equation 13 relative to Equation 1a. Test data from the following sources were included in this analysis: Fielding and Huang (1971); Krawinkler et al. (1971); Bertero et al. (1973); Becker (1975); Popov et al. (1986); Ghobarah, Korol and Osman (1992); Tsai, Wu and Popov (1995); FEMA (1997); Choi et al. (2000); Lee, Stojadinovic, Goel,

Table 5. Parameters for Tests Used to Evaluate Panel Zone Nominal Strength							
Test Designation	$F_{y,web}$ (ksi)	t_p (in.)	t_{cf} (in.)	b_{cf} (in.)	d_g (in.)	d_c (in.)	Axial (Y/N)
Fielding and Huang	31.4	0.84	1.378	15.66	24.72	15.38	Y
Krawinkler et al.: A-1	41.0	0.245	0.398	5.82	10.0	7.93	Y
Krawinkler et al.: A-2	41.0	0.245	0.398	5.82	10.0	7.93	Y
Krawinkler et al.: B-2	47.0	0.575	0.933	8.29	13.72	9.0	Y
Bertero et al.: A-3	44.7	0.495	0.398	5.82	10.0	7.93	Y
Bertero et al.: B-3	47.0	0.575	0.933	8.29	11.96	9.0	Y
Bertero et al.: B-4	47.0	0.575	0.933	8.29	10.22	9.0	Y
Becker: 1	40.6	0.875	0.645	9.995	13.89	13.89	N
Becker: 2	40.6	0.375	0.645	9.995	13.89	13.89	N
Popov et al.: 2	49.0	0.5625	0.625	8.25	17.9	18.0	Y
Popov et al.: 3	49.0	1.0625	1.25	8.5	18.75	19.125	Y
Popov et al.: 4	49.0	1.0625	1.25	8.5	18.75	19.125	Y
Popov et al.: 6	49.0	0.6875	1.25	8.5	18.75	19.125	Y
Popov et al.: 7	60.0	0.955	0.93	8.42	18.47	21.62	Y
Popov et al.: 8	60.0	0.955	0.93	8.42	18.47	21.62	Y
Ghobarah et al.: CB-1	52.2	0.305	0.53	7.995	14.1	13.66	Y
Ghobarah et al.: CC-3	47.3	0.515	0.81	12.125	16.01	12.53	Y
Tsai et al.: TH2	56.6	0.745	1.19	15.565	21.43	14.98	N
FEMA: EERC-PN1	49.5	0.83	1.31	15.65	29.65	15.22	N
FEMA: EERC-PN2	53.5	0.83	1.31	15.65	29.65	15.22	N
FEMA: EERC-PN3	56.0	0.83	1.31	15.65	29.65	15.22	N
FEMA: EERC-AN1	56.0	0.83	1.31	15.65	31.275	15.22	N
FEMA: UCSD-1	51.2	0.83	1.31	15.65	29.65	15.22	N
FEMA: UCSD-2	51.2	0.83	1.31	15.65	29.65	15.22	N
FEMA: UCSD-3	51.2	0.83	1.31	15.65	29.65	15.22	N
FEMA: UCB-PN1	53.5	1.175	1.89	15.995	35.85	16.38	N
FEMA: UCB-RN2	53.5	1.175	1.89	15.995	45.60	16.38	N
FEMA: UCB-RN3	53.5	1.175	1.89	15.995	35.85	16.38	N
FEMA: UCB-AN1	50.0	1.175	1.89	15.995	44.85	16.38	N
FEMA: UTA-4	53.5	1.175	1.89	15.995	37.85	16.38	N
Choi et al.: SP-9.1	57.0	0.830	1.31	15.65	29.65	15.22	N
Choi et al.: SP-10.1	59.0	1.175	1.89	15.995	30.17	16.38	N
Choi et al.: SP-10.2	59.0	1.675	1.89	15.995	30.17	16.38	N
Lee et al.: SP-3.1	49.8	0.59	0.94	14.67	23.73	14.48	N
Lee et al.: SP-3.2	49.8	0.59	0.94	14.67	23.73	14.48	N

Table 5 (continued). Parameters for Tests Used to Evaluate Panel Zone Nominal Strength							
Test Designation	F_{yc} (ksi)	t_p (in.)	t_{cf} (in.)	b_{cf} (in.)	d_g (in.)	d_c (in.)	Axial (Y/N)
Lee et al.: SP-4.1	48.3	0.68	1.09	15.5	29.65	14.78	N
Lee et al.: SP-4.2	48.3	0.68	1.09	15.5	29.65	14.78	N
Lee et al.: SP-5.1	51.3	0.83	1.31	15.65	29.65	15.22	N
Lee et al.: SP-7.2	44.2	1.175	1.89	15.995	35.85	16.38	N
Ricles et al.: LU-T1	49.2	1.41	2.26	16.23	35.85	17.12	N
Ricles et al.: LU-T2	49.2	1.41	2.26	16.23	35.85	17.12	N
Ricles et al.: LU-T4	49.2	1.41	2.26	16.23	35.85	17.12	N
Ricles et al.: LU-C1	54.0	3.27	2.845	16.59	35.85	18.29	N
Ricles et al.: LU-C2	54.0	3.27	2.845	16.59	35.85	18.29	N
U. of Minnesota: CR1	52.3	1.29	2.07	16.11	24.31	16.74	N
U. of Minnesota: CR2	54.0	1.515	1.44	15.71	24.31	15.48	N
U. of Minnesota: CR3	57.5	1.83	1.31	15.65	24.31	15.22	N
U. of Minnesota: CR4R	56.8	2.33	1.31	15.65	24.31	15.22	N
U. of Minnesota: CR5	58.7	1.93	1.09	15.5	24.31	14.78	N

Margarian, Choi, Wongkaew, Reyher and Lee (2000); and Ricles, Mao, Kaufmann and Fisher (2000). A total of 49 tests, including the five cruciform specimens tested in the present research, that exceeded the design deformation of $4\gamma_y$ in the panel zones were included, as the experimental shear force at this deformation level is required for the comparison. Tables 4 and 5 tabulate the relevant parameters from all tests included in the following analysis. The reported yield stress is the coupon yield stress, or otherwise the dynamic yield stress from the mill reports. The collection of tests represents a wide range of parameters. Nominal steel yield strengths of 36 and 50 ksi are included, with a range of measured column yield strengths from 31.4 to 60.0 ksi. Column sizes range from W8 sections to W21 sections, while girder sizes range from W10 sections to W36 sections. Several tests were stiffened with doubler plates and/or continuity plates, and some haunched, cover-plated, and end-plate connections are also included. Panel zone thicknesses range from 0.245 to 3.27 in., and column flange thicknesses range from 0.398 to 2.845 in. Most tests conducted prior to the Northridge earthquake included compressive column axial loads, while none of the post-Northridge tests were axially loaded. With the exception of the tests by Fielding and Huang (1971) and Becker (1975), the girders of the specimens were cyclically loaded. Lee et al. (2002) discuss how the experimental shear force at $4\gamma_y$ was determined for each test.

Predicted panel zone strengths, R_v, were calculated using Equation 1a (AISC, 2002) and the proposed Equation 13. No resistance factors were included (in other words, $\phi_v = 1.0$). For the calculation of panel zone strengths, measured material properties were used. Table 6 presents the resulting test-to-predicted ratios (V_{pz}/R_v). Also tabulated are the increases beyond yield incorporated in each equation. These post-yield contributions are defined in each equation by the second term in parentheses, and represent the effects of the panel zone boundary elements (primarily the column flanges) following panel zone yielding. As Table 6 shows, Equation 13 better predicted the panel zone shear strength for the group of tests analyzed. The mean test-to-predicted ratio was 1.060, as compared with a mean of 0.856 for Equation 1a. The standard deviations for both methods were comparable. In all cases, however, a lower strength increase beyond yielding is predicted by Equation 13.

An important observation arises when comparing the test-to-predicted ratios of tests with W14 and larger columns to those with W12 and smaller columns. For those tests with W14 and larger columns, the mean test-to-predicted ratio is 0.812 for Equation 1a and 1.012 for Equation 13. When tests with W12 and smaller columns are considered, the mean test-to-predicted ratio increases to 1.005 for Equation 1a and 1.226 for Equation 13. This suggests that the AISC (2002) provisions (Equation 1a) are satisfactory for smaller

Table 6. Panel Zone Strength Test-to-Predicted Ratios				
Test Designation	V_{pz}/R_v (Eqn. 1a)	V_{pz}/R_v (Eqn. 13)	Post-Elastic (Eqn. 1a)	Post-Elastic (Eqn. 13)
Fielding and Huang	0.781	1.011	0.279	0.078
Krawinkler et al.: A-1	0.996	1.208	0.142	0.028
Krawinkler et al.: A-2	0.904	1.095	0.142	0.028
Krawinkler et al.: B-2	0.946	1.220	0.305	0.104
Bertero et al.: A-3	0.913	1.051	0.070	0.014
Bertero et al.: B-3	1.020	1.322	0.350	0.136
Bertero et al.: B-4	1.091	1.413	0.409	0.187
Becker: 1	0.645	0.743	0.074	0.017
Becker: 2	0.740	0.911	0.172	0.040
Popov et al.: 2	1.090	1.241	0.053	0.009
Popov et al.: 3	0.929	1.082	0.105	0.035
Popov et al.: 4	0.923	1.075	0.105	0.035
Popov et al.: 6	1.106	1.330	0.162	0.054
Popov et al.: 7	0.708	0.805	0.057	0.014
Popov et al.: 8	0.713	0.811	0.057	0.014
Ghobarah et al.: CB-1	1.062	1.264	0.115	0.022
Ghobarah et al.: CC-3	1.142	1.450	0.231	0.058
Tsai et al.: TH2	0.835	1.080	0.276	0.077
FEMA: EERC-PN1	0.803	1.016	0.215	0.048
FEMA: EERC-PN2	0.790	1.000	0.215	0.048
FEMA: EERC-PN3	0.740	0.936	0.215	0.048
FEMA: EERC-AN1	0.715	0.901	0.204	0.043
FEMA: UCSD-1	0.776	0.982	0.215	0.043
FEMA: UCSD-2	0.826	1.045	0.215	0.043
FEMA: UCSD-3	0.809	1.024	0.215	0.043
FEMA: UCB-PN1	0.789	1.008	0.248	0.065
FEMA: UCB-RN2	0.783	0.981	0.195	0.040
FEMA: UCB-RN3	0.789	1.008	0.248	0.065
FEMA: UCB-AN1	0.832	1.044	0.199	0.042
FEMA: UTA-4	0.781	0.994	0.235	0.059
Choi et al.: SP-9.1	0.844	1.069	0.215	0.048
Choi et al.: SP-10.1	0.748	0.967	0.295	0.092
Choi et al.: SP-10.2	0.688	0.851	0.207	0.065
Lee et al.: SP-3.1	1.068	1.338	0.192	0.038
Lee et al.: SP-3.2	1.090	1.365	0.192	0.038
Lee et al.: SP-4.1	1.017	1.272	0.185	0.034
Lee et al.: SP-4.2	0.986	1.234	0.185	0.034
Lee et al.: SP-5.1	0.910	1.152	0.215	0.048
Lee et al.: SP-7.2	0.921	1.178	0.248	0.065

Table 6 (continued). Panel Zone Strength Test-to-Predicted Ratios				
Test Designation	V_{pz}/R_v (Eqn. 1a)	V_{pz}/R_v (Eqn. 13)	Post-Elastic (Eqn. 1a)	Post-Elastic (Eqn. 13)
Ricles et al.: LU-T1	0.807	1.040	0.287	0.091
Ricles et al.: LU-T2	0.798	1.028	0.287	0.091
Ricles et al.: LU-T4	0.851	1.096	0.287	0.091
Ricles et al.: LU-C1	0.729	0.879	0.188	0.075
Ricles et al.: LU-C2	0.783	0.944	0.188	0.075
U. of Minnesota: CR1	0.752	0.981	0.394	0.168
U. of Minnesota: CR2	0.787	0.956	0.171	0.051
U. of Minnesota: CR3	0.711	0.840	0.119	0.032
U. of Minnesota: CR4R	0.697	0.812	0.093	0.025
U. of Minnesota: CR5	0.764	0.885	0.080	0.018
Mean	0.856	1.060		
Standard Deviation	0.132	0.170		

columns and somewhat unconservative for larger columns. These provisions were developed from the results of testing by Krawinkler et al. (1971) and Bertero et al. (1973) on W8 column sections. Equation 13, on the other hand, was more accurate in its prediction of the panel zone strength of larger columns and appears somewhat conservative for smaller columns. These results suggest that Equation 13 better predicts panel zone behavior in joints with member sizes commonly used in current seismic moment frame construction.

A resistance factor was also calculated for Equation 13 using the data from the group of 49 tests and the procedure given by Equation C-A5–4 in the commentary of AISC (1999b). The referenced equation computes an approximate resistance factor based on the mean and nominal resistances, the coefficient of variation of the resistance, and a reliability index. A reliability index of 2.6 was selected, consistent with the typical value specified for members (AISC, 1999b). Using the mean test-to-predicted ratio of 1.060 and corresponding coefficient of variation equal to 0.160, a resistance factor of 0.86 was calculated; using a value of 0.85 for design would then be reasonable.

Lee et al. (2002) compare the panel zone thicknesses resulting from Equations 1 and 13 and from the panel zone design procedure put forward in FEMA (2000a) for a wide range of interior and exterior connections. The results (not presented here) show that the panel zone strength proposed in Equation 13 typically requires thicker panel zones than AISC (1992), AISC (1997a), AISC (2000), AISC (2002), and FEMA (2000a). The FEMA (2000a) panel zone thicknesses were also often found to be smaller than the panel zone thicknesses required from AISC (2002), even for columns with thick flanges. If it is assumed that the AISC (2002) and FEMA (2000a) procedures result in adequate panel zone designs, use of Equation 13 should also include adoption of a lower panel zone shear required strength (in other words, panel zone shear demand) to result in similar panel zone thicknesses.

PANEL ZONE REQUIRED STRENGTH BASED ON $8\gamma_y$

The results of the tests conducted for this research also indicate that a panel zone strength design procedure that does not target a panel zone shear deformation of $4\gamma_y$ may be a reasonable design alternative, as the connections tested in this work with weak panel zones performed well. As shown in Figure 4, γ/γ_y values over 10 were developed in several specimens. The panel zone of Specimen CR4R, which had the largest panel zone design capacity/demand ratio in this research program [in other words, $\phi_v R_v/R_u = 0.93$ as per AISC (2002)], developed the smallest shear deformation of $\gamma/\gamma_y \approx 6$ at 4.0% drift level. By removing the $4\gamma_y$ limitation, however, it can be seen in Figures 4a through 4e that the nominal panel zone design strength, R_v, from Equation 1a, using the specified minimum yield stress of the column and $\phi_v = 1.0$, satisfactorily estimates the panel zone ultimate strength in the WUF-W steel moment connections that have

weaker panel zones. The only exception is Specimen CR4R. Due to the limited panel zone shear deformation associated with the stronger panel zone, the backbone curve of Specimen CR4R could not reach the shear strength predicted by Equation 1a.

The results presented in Figures 4a through 4c indicate that by permitting more panel zone shear deformation, Equation 1a can be used for the panel zone design of WUF-W moment connections that have weaker panel zones as per AISC (2002). For practical application, however, the maximum acceptable panel zone shear deformation has to be decided upon, and the panel zone required strength (in other words, the panel zone design demand) must be appropriately scaled. These two issues are discussed herein based on the experimental cyclic panel zone behavior of the first three WUF-W specimens (Specimens CR1, CR2 and CR3). The experimental results of Specimens CR4R and CR5 are excluded in these discussions because of the inconsistent cyclic connection response associated with the much stronger panel zone (as compared with the other panel zones) in Specimen CR4R and because of the significant deviation from the SCWB criteria of AISC (2002) in Specimen CR5.

It has been suggested that one major effect of large panel zone distortion in steel moment connections is the local kink that occurs in the column flanges at the level of the girder flanges (Krawinkler et al., 1971; Krawinkler, 1978; Popov et al., 1986; Roeder and Foutch, 1996; El-Tawil et al., 1999; El-Tawil, 2000; Mao et al., 2001; Wongkaew et al., 2001; Roeder, 2002). This local kinking phenomenon has been hypothesized to significantly affect the seismic performance of the steel moment connections during the Northridge earthquake. Experiments by Krawinkler et al. (1971), Krawinkler (1978), and Popov et al. (1986) revealed the effects of excessive panel zone distortion. The kinks in the column flanges caused high local stress and strain demands in the girder flange-to-column flange junction area, which led to the low-cycle fatigue cracking in the groove welds.

Analytical studies by El-Tawil et al. (1999), El-Tawil (2000) and Chi, Deierlein and Ingraffea (2000) also predicted the effects of large panel zone deformations. Based on finite element analyses, El-Tawil et al. (1999) and El-Tawil (2000) showed that a weak panel zone could lead to a greater potential for brittle fracture and/or low-cycle fatigue in the connection at higher plastic rotations. Chi et al. (2000) also showed that the weld toughness demand of the girder flange dramatically increased for the case of weak panel zones. Another analytical study by Mao et al. (2001) indicated that the deformations in a weak panel zone could increase the potential for low-cycle fatigue cracking at the edge of girder web-to-column flange groove welds (in other words, at the shear tab) in the WUF-W connection detail. An experimental study by Ricles et al. (2002) confirmed these findings by Mao et al. (2001).

There was limited low-cycle fatigue cracking at the top or bottom edge of the shear tab in all specimens that typically initiated during the 4.0% interstory drift cycles (and the 2.0% interstory drift cycles for Specimen CR5), and this occurrence could be interpreted as supporting the observations by Mao et al. (2001) and Ricles et al. (2002). It may be reasonable to assume then that the large panel zone deformation and the associated kink of the column flange did contribute to the cracking at the edge of the shear tab in the tested WUF-W specimens. However, the failure mode ultimately was low-cycle fatigue cracking in the girder flange-to-column flange groove welds (Lee et al., 2002, 2005). Furthermore, no significant strength degradation in the connection was recorded until the girder flanges were locally buckled or until the low-cycle fatigue crack in the girder flange was significant after several 4.0% drift cycles. Hence, it cannot be concluded that the local low-cycle fatigue cracking in the edge of the shear tab contributed to strength degradation in the tested WUF-W specimens. Fracturing in the edges of the shear tab or its associated welds seemed to be more directly affected by girder flange local buckling, low-cycle fatigue crack opening in the girder flanges, or both, under large connection deformations (Lee et al., 2005). The cracking in the edge of the shear tab, however, might increase the stress and strain demands in girder flanges at higher drift levels, although this increase is believed to be insignificant.

The experimental investigation in this study showed that with the presently specified WUF-W connection and access hole details and notch-tough weld material, adequate connection performance can be achieved in the WUF-W moment connections even in the presence of higher stress and strain demands due to a weaker panel zone. Specimens CR1, CR2 and CR3 completed SAC loading history up to 4.0% drift cycles without losing any connection strength even under panel zone shear deformations much larger than $4\gamma_y$.

In fact, the good performance of Specimen CR1 is even more significant considering that the girder flange-to-column flange CJP groove welds in Specimen CR1 were made with a $^5/_{64}$-in.-diameter NR-305 wire and weld procedures that unintentionally produced weld metal with only 2 to 3 ft-lb at 0 °F and an average of 19 ft-lb at 70 °F; in other words, it did not meet the FEMA (2000a) recommended minimum notch toughness requirements (Lee et al., 2002, 2005). [This was also a problem with Specimen CR4, which did result in brittle fracture, as discussed in Lee et al. (2002, 2005); the weld metal in the remaining specimens met the FEMA (2000a) recommended minimum notch toughness requirements.] Therefore, the good performance of Specimen CR1 indicates that excessive panel zone deformation does not necessarily increase the potential for brittle fracture.

Based on the cyclic panel zone behavior of the WUF-W specimens tested in this research and an experimental study of the Free-Flange moment-resisting connection detail

tested by Choi et al. (2000), a possible new seismic panel zone shear required strength calculation is suggested for steel-resisting moment connections that exhibit a similar flow of forces from the girder to the column as the WUF-W or Free-Flange connections and in which a maximum panel zone shear deformation of more than $4\gamma_y$ would be permitted. For the development of this new required strength, an acceptable maximum panel zone shear deformation is decided upon, first based on the experimental results of Specimens CR1, CR2, and CR3 and the experimental results of one Free-Flange specimen [Specimen SP 9.1 (Choi et al., 2000)] that had a similar panel zone design capacity/demand ratios (in other words, $\phi_v R_v/R_u \approx 0.7$) as per AISC (2002). Secondly, the panel zone design demands calculated from a modified approach from AISC (1999c) are scaled to the cyclic panel zone results of these tests.

Several other moment-resisting connections tested in the literature that have had underdesigned panel zones have also shown good cyclic performance and high ductility. Two Free-Flange connections of Choi et al. (2000) (in other words, Specimens SP 9.1 and SP 10.1) showed good cyclic performance without significant strength degradation up to several 5.0% interstory drift cycles in Specimen SP 9.1 and up to five 4.0% interstory drift cycles in Specimen SP 10.1. Specimen SP 9.1, which had a nominal value for $\phi_v R_v/R_u$ of 0.74 as per AISC (2002), developed more than $12\gamma_y$ maximum panel zone shear deformation during the 5.0% interstory drift cycles. The panel zone shear deformation of Specimen SP 9.1 at the 4.0% interstory drift level was approximately $10\gamma_y$, an amount very similar to the maximum panel zone shear deformation developed in the WUF-W specimens CR1, CR2, and CR3 during the 4.0% drift cycles. The maximum panel zone shear deformation of Specimen SP 10.1 ($\phi_v R_v/R_u = 0.94$) at the 4.0% interstory drift level was approximately $8.5\gamma_y$ when the loading on the girder was applied in one direction, while the loading applied in the other direction developed a maximum panel zone shear deformation of approximately $10\gamma_y$. In this study, $8\gamma_y$ is thus suggested for the permissible maximum panel zone shear deformation in steel moment-resisting connections that exhibit a similar flow of forces from the girder to the column as the WUF-W or Free-Flange connections. This $8\gamma_y$ limitation was also selected as the maximum shear deformation in the analytical model of the panel zone inelastic behavior recently suggested by Wongkaew et al. (2001) after the study of the cyclic panel zone behavior of several Free-Flange specimens.

To design panel zone thicknesses corresponding to the same or similar cyclic performance as WUF-W Specimens CR1, CR2, and CR3 and Free-Flange Specimen SP 9.1, the panel zone shear required strength calculated from AISC (1999c) (modified by using $\phi_v = 1.0$ and removing the factor of 0.8 from the girder moments) should be adjusted. Specifically, the panel zone shear required strengths for the preceding four girder-to-column combinations should be downscaled by a factor of 0.72 (CR1), 0.66 (CR2), 0.74 (CR3), and 0.74 (SP9.1) (calculated in a manner similar to Table 2), respectively, to achieve the corresponding panel zone thicknesses tested in those four specimens. However, these required strength scale factors cannot be directly used for the panel zone design of steel moment-resisting connections. This is because the target panel zone shear deformation was adjusted to $8\gamma_y$, instead of the values of $10\gamma_y$ or more that were observed in these four specimens. In this study, a scale factor of 0.85 is thus suggested from the comparison of the developed maximum panel zone shear deformations between Specimen CR3 and Specimen CR4R. These two specimens consisted of the same girder and column sections, with the major difference being the column stiffener details [Specimen CR3 used fillet-welded continuity plates; Specimen CR4R used a box (offset) doubler plate detail welded with complete-joint-penetration groove welds (Lee et al., 2002, 2005)]. Specimen CR3, which had $\phi_v R_v/R_u = 0.74$ as per AISC (2002), developed more than $10\gamma_y$ panel zone shear deformation during 4.0% interstory drift cycles, while only approximately $6\gamma_y$ was developed at the same interstory drift level in Specimen CR4R (which had $\phi_v R_v/R_u = 0.93$ per the same provisions). By ignoring the effects of the column stiffener detailing on the cyclic panel zone behavior, it is reasonable to choose 0.85 (in other words, approximately the average between 0.74 and 0.93) as the scale factor of the panel zone shear required strength, targeting $8\gamma_y$ as the maximum panel zone shear deformation.

The resulting panel zone shear required strength, R_u^*, can be expressed as

$$R_u^* = 0.85\left(\sum_{girders}\frac{1.1R_yF_{yg}Z_g + V_g a}{0.95d_g} - V_c\right) \qquad (14)$$

where

R_y = ratio of expected yield stress of girder to specified minimum value
F_{yg} = specified minimum yield stress of the girder
Z_g = girder plastic section modulus
V_g = shear force in the girder at plastic hinge location
a = distance from column face to girder plastic hinge location

The ratios of capacity from Equation 1a (AISC, 2002) to demand from Equation 14 are shown in Table 2. It is seen that the specimens designed in this work, with the exception of Specimen CR4R, would still require a larger panel zone thickness, but not as severe as the criteria of AISC (2002).

Note that for connections with weak panel zones, in other words, for connections designed using Equation 14 to compute required strength, it may be appropriate for the plastic

hinge location to be assessed at the column face rather than a distance of half the girder depth away from the column face. For this case, the 0.85 scale factor should be changed to 0.95 in Equation 14; the associated required strengths would then be similar in magnitude.

The resulting panel zone required strength of Equation 14 is more economical, and the associated welding of thinner stiffeners may decrease the potential for fabrication cracking in the *k*-area of the column (Tide, 2000; Lee et al., 2002, 2005; Hajjar et al., 2003).

Finally, Equation 14 may be considered for use in conjunction with Equation 13 for connections that exhibit a similar flow of forces from the girder to the column as the WUF-W or Free-Flange connections. It was indicated that a smaller required strength should be used with Equation 13 if one wants to obtain panel zone thicknesses that are similar to those obtained from AISC (2002), but through using the more accurate assessment of panel zone strength presented in Equation 13. The ratios of capacity from Equation 13 to demand from Equation 14 are shown in Table 2. It is seen that, through the use of these two equations, the specimens designed in this work would yield panel zone thickness approximately the same as through the use of AISC (2002), as the capacity-to-demand ratios are similar. The exception is Specimen CR1, which has thick column flanges and whose strength is overestimated considerably by Equation 1a. However, further research is recommended to determine the best required strength to associate with the use of Equation 13.

CONCLUSIONS AND SUGGESTIONS

This study investigated the cyclic panel zone behavior of five full-scale Welded Unreinforced Flange-Welded Web (WUF-W) cruciform specimens that had weak panel zones as compared to those required by AISC (2002). The experimental setup and general performance of these connections is reported in a companion paper (Lee et al., 2005). Major findings in this study and several conclusions and suggestions are summarized in the following.

1. The five WUF-W cruciform specimens tested in this work, which had weaker panel zones as compared with those required by the 2002 AISC Seismic Provisions (AISC, 2002), performed satisfactorily when subjected to the SAC (1997) loading history. Each specimen completed 14 (Specimen CR1), 16 (CR2), 14 (CR3), 12 (CR4R), and 6 (CR5) cycles at 4.0% interstory drift, respectively, without any significant fracturing or strength degradation in the connection. Visible cracking in the connections typically first occurred at the toe of the fillet welds that reinforced the topside of these CJP welds in the 3.0% interstory drift cycles in some specimens, but the connections suffered no strength degradation until the girder flanges were locally buckled or until the low cycle fatigue cracks in the girder flange were significant after several 4.0% drift cycles. The first three specimens (Specimens CR1, CR2, and CR3) developed more than $10\gamma_y$ of panel zone shear deformation during the 4.0% interstory drift cycles, while the other two specimens developed more than $6\gamma_y$ (Specimen CR4R) and approximately $8\gamma_y$ (Specimen CR5) maximum panel zone shear deformations at the same interstory drift level. These experimental results indicate that, with the appropriate connection detailing and the use of notch-tough weld metal, more than $4\gamma_y$ may be assumed as the acceptable maximum panel zone shear deformation in steel moment-resisting connections that exhibit a similar flow of forces from the girder to the column as the WUF-W or Free-Flange connections, even in the presence of higher stress and strain demands due to weaker panel zones.

2. While the plastic moment was achieved in the five WUF-W specimens tested in this work, no full-depth girder plastic hinge formation was observed up to the 4.0% interstory drift cycles. With the weaker panel zones in these five specimens, a major portion of the girder yielding was observed near the girder flange-to-column flange junction area even in Specimens CR1 and CR2, which satisfied the Strong Column-Weak Beam (SCWB) criteria of the 2002 AISC Seismic Provisions (AISC, 2002). The girder webs yielded only locally at the higher interstory drift cycles, just before the low cycle fatigue fracturing in the girder flange-to-column flange groove welds occurred in all specimens. Observation of the yielding in the joint region at the higher interstory drift levels indicated that it is more realistic to calculate the panel zone required strength directly at the column face for connections that have weaker panel zones, without considering the moment increments due to the girder shear force at the assumed girder plastic hinge location.

3. When compared with the 1992 AISC Seismic Provisions (AISC, 1992), the 2002 AISC Seismic Provisions (AISC, 2002) require much stronger panel zones. This is because the calculated girder moment of 2002 AISC Seismic Provisions (AISC, 2002) that is used to assess panel zone required strength would normally be increased by a factor of approximately 1.4 as compared with the typical value of panel zone required strength that was calculated from the 1992 AISC Seismic Provisions (AISC, 1992); this factor considers the probable girder plastic moment and the additional moment due to the shear amplification.

4. The AISC seismic panel zone shear strength equation from the 2002 AISC Seismic Provisions (AISC, 2002) (Equation 1a, with $\phi_v = 1.0$) overestimated the panel zone shear strengths in the WUF-W specimens tested in this work when compared with the experimental panel zone

responses at $4\gamma_y$ of shear deformation, which is implied (at least approximately) in Equation 1a as the design shear deformation of the panel zone. A new panel zone design shear strength equation (Equation 13) is thus presented and compared to the results from this work and to other experiments from the literature that have a wide range of panel zone characteristics. The new equation provided a more accurate prediction of panel zone strength. A resistance factor of 0.85 is recommended for use with the equation.

5. Alternately, by removing the $4\gamma_y$ limitation, the AISC seismic panel zone shear strength equation (AISC, 2002) satisfactorily estimated the panel zone strengths at larger panel zone shear deformations. These experimental results indicate that, by permitting more panel zone shear deformation, the AISC seismic panel zone equation (AISC, 2002) may also be used for the panel zone design of steel moment-resisting connections (that exhibit a similar flow of forces from the girder to the column as the WUF-W or Free-Flange connections) even though they have weaker panel zones as per the 2002 AISC Seismic Provisions (AISC, 2002). As such, based on experimental results of the first three WUF-W specimens (in other word, Specimens CR1, CR2 and CR3) tested in this research and a Free-Flange specimen tested at the University of Michigan, a new panel zone shear required strength equation, Equation 14, was proposed for use with the WUF-W and similar connections that are to be designed with weaker panel zones. In this new panel zone design criterion, the 2002 AISC seismic panel zone design equation (AISC, 2002) presented in Equation 1a (with $\phi_v = 1.0$) is used, but the target panel zone shear deformation at the peak shear strength is presumed to be $8\gamma_y$ rather than $4\gamma_y$. Equation 14 was obtained by using the panel zone shear required strength originally calculated from AISC (1999c) (modified by using $\phi_v = 1.0$ and removing the factor of 0.8 from the girder moments), scaled down to 85% of its original value based on the experimental results of the preceding four specimens. Furthermore, it is proposed that this 0.85 scale factor could be adjusted to 0.95 if the girder plastic hinge is assumed to form at the column face for the calculation of panel zone required strength. Using the panel zone shear required strength calculated from Equation 14 and using the panel zone shear strength of AISC (2002) requires moderately stronger panel zones in steel moment-resisting connections as compared to the 1992 AISC Seismic Provisions (AISC, 1992). It should be noted, however, that the presence of large axial compression forces, which has not been studied in this work, should be considered in the design, and the influence of large panel zone deformations should be considered in the assessment of the structural stability of the steel frame.

6. If used with the panel zone shear required strength of AISC (2002), Equation 13 likely provides thicker panel zones than the design procedure of AISC (2002). Alternately, using the panel zone nominal strength calculation of AISC (2002) in conjunction with the alternative panel zone required strength of Equation 14 provides more economical results, but the nominal strength calculation remains less accurate than Equation 13. Use of Equation 13 to compute panel zone nominal strength and Equation 14 to compute panel zone shear required strength is proposed for consideration for WUF-W and similar connections. However, future work should be conducted to investigate more comprehensively the corresponding panel zone shear required strength that is best used in conjunction with Equation 13. In addition, the proposed panel zone design criteria for steel moment-resisting connections were developed based predominantly on the experimental results of W14 column sections. To expand these design criteria to deeper column sections, further experimental research is required.

ACKNOWLEDGMENTS

This research was sponsored by the American Institute of Steel Construction, Inc., and by the University of Minnesota. In-kind funding and materials were provided by LeJeune Steel Company, Minneapolis, Minnesota; Danny's Construction Company, Minneapolis, Minnesota; Braun Intertec, Minneapolis, Minnesota; Nucor-Yamato Steel Company, Blytheville, Arkansas; Lincoln Electric Company, Cleveland, Ohio; and Edison Welding Institute, Cleveland, Ohio. Supercomputing resources were provided by the Minnesota Supercomputing Institute. The authors wish to thank Professor T.V. Galambos, Mr. P.M. Bergson, Ms. S.D. Ojard, Mr. D. Webster, and Ms. A. Kingsley of the University of Minnesota, Mr. L.A. Kloiber of LeJeune Steel Company, and the members of the external advisory committee on this project for their valuable assistance.

While this paper was under review, co-author Robert Dexter passed away unexpectedly in November 2004. Dr. Dexter was known nationally and internationally for his work on fracture and fatigue of steel structures. His sudden death cut short a rising career in applied steel research, one that influenced an unusually wide number of areas, including fracture problems in buildings, fatigue in bridges, cracking in ship panels, and collapse of overhead highway signs. He contributed extensively to the writing of the AISC Specification, the AASHTO steel bridge design specification, the RCSC bolt specification, and the AWS welding specification. His contributions to the research reported in this paper were integral throughout the project. He will be greatly missed by his colleagues around the world.

REFERENCES

AISC (1992), *Seismic Provisions for Structural Steel Buildings*, American Institute of Steel Construction, Inc., Chicago, IL.

AISC (1997a), *Seismic Provisions for Structural Steel Buildings*, American Institute of Steel Construction, Inc., Chicago, IL.

AISC (1997b), "AISC Advisory on Mechanical Properties Near the Fillet of Wide Flange Shapes and Interim Recommendations, January 10, 1997," *Modern Steel Construction*, American Institute of Steel Construction, Inc., Chicago, IL, February, p. 18.

AISC (1999a), *Seismic Provisions for Structural Steel Buildings—Supplement No. 1*, American Institute of Steel Construction, Inc., Chicago, IL.

AISC (1999b), *Load and Resistance Factor Design Specification for Structural Steel Buildings*, American Institute of Steel Construction, Inc., Chicago, IL.

AISC (1999c), *Stiffening of Wide-Flange Columns at Moment Connections: Wind and Seismic Applications*, Design Guide No. 13, American Institute of Steel Construction, Inc., Chicago, IL.

AISC (2000), *Seismic Provisions for Structural Steel Buildings—Supplement No. 2*, AISC, Chicago, IL.

AISC (2002), *Seismic Provisions for Structural Steel Buildings*, AISC, Chicago, IL.

ASCE (1995), "Minimum Design Loads for Buildings and Other Structures," ANSI/ASCE 7-95, American Society of Civil Engineers, Reston, VA.

Bertero, V.V., Krawinkler, H., and Popov, E. P. (1973), *Further Studies on Seismic Behavior of Steel Beam-Column Subassemblages*, Report No. EERC-73/27, Earthquake Engineering Research Center, University of California, Berkeley, CA.

Becker, R. (1975), "Panel Zone Effect on the Strength and Stiffness of Steel Rigid Frames," *Engineering Journal,* AISC, Vol. 12, No. 1, pp. 19–29.

Biddah, A. and Heidebrecht, A.C. (1998), "Seismic Performance Moment-Resisting Steel Frame Structures Designed for Different Levels of Seismic Hazard," *Earthquake Spectra,* EERI, Vol. 14, No. 4, pp. 597–627.

Biddah, A. and Heidebrecht, A.C. (1999), "Evaluation of the Seismic Level of Protection Afforded to Steel Moment Resisting Frame Structures Designed for Different Design Philosophies," *Canadian Journal of Civil Engineering,* Vol. 26, pp. 35–54.

Bjorhovde, R. Goland, L. J., and Benac, D. J. (1999), "Tests of Full-Scale Beam-to-Column Connections," Southwest Research Institute, San Antonio, TX.

Charney, F.A. and Johnson, R. (1986), "The Effect of Panel Zone Deformations on the Drift of Steel Framed Structures," Proceedings of the Fourth ASCE Structures Congress '86, ASCE, Reston, VA.

Chi, W., Deierlein, G. G., and Ingraffea, A. (2000), "Fracture Toughness Demands in Welded Beam-Column Moment Connections," *Journal of Structural Engineering*, ASCE, Vol. 126, No. 1, pp. 88–97.

Choi, J., Stojadinovic, B., and Goel, S.C. (2000), *Development of Free Flange Moment Connection,* Report No. UMCEE 00-15, Department of Civil and Environmental Engineering, University of Michigan, Ann Arbor, MI.

El-Tawil, S., Vidarsson, E., Mikesell, T., and Kunnath, S.K. (1999), "Inelastic Behavior and Design of Steel Panel Zones," *Journal of Structural Engineering*, ASCE, Vol. 125, No. 2, pp. 183–193.

El-Tawil, S. (2000), "Panel Zone Yielding in Steel Moment Connections," *Engineering Journal*, AISC, Vol. 37, No. 1, pp. 120–131.

Federal Emergency Management Agency (FEMA) (1997), "Connection Test Summaries," Report No. FEMA 289, Federal Emergency Management Agency, Washington, D.C.

FEMA (2000a), *Recommended Seismic Design Criteria for New Steel Moment-Frame Buildings*, Report No. FEMA 350, Federal Emergency Management Agency, Washington, D.C.

FEMA (2000b), *State of the Art Report on Connection Performance*, Report No. FEMA 335D, Federal Emergency Management Agency, Washington, D.C.

Fielding, D.J. and Huang, J.S. (1971), "Shear in Steel Beam-to-Column Connections," *Welding Journal,* AWS, Vol. 50, No. 7, Research Supplement, pp. 313–326.

Ghobarah, A., Korol, R.M., and Osman, A. (1992), "Cyclic Behavior of Extended End-Plate Joints," *Journal of Structural Engineering,* ASCE, Vol. 118, No. 5, pp. 1333–1353.

Hajjar, J.F., Dexter, R.J., Ojard, S.D., Ye, Y., and Cotton, S.C. (2003), "Continuity Plate Detailing for Steel Moment-Resisting Connections," *Engineering Journal,* AISC, Vol. 40, No, 4, pp. 189–211.

Jones, S.L., Fry, G.T., and Engelhardt, M.D. (2002), "Experimental Evaluation of Cyclically Loaded Reduced Beam Section Moment Connections," *Journal of Structural Engineering,* ASCE, Vol. 128, No. 4, pp. 441–451.

Kim, K.D. and Engelhardt, M.D. (2002), "Monotonic and Cyclic Loading Models for Panel Zones in Steel Moment Frames," *Journal of Constructional Steel Research*, Vol. 58, Nos. 5–8, pp. 605–635.

Krawinkler, H., Bertero, V.V., and Popov, E.P. (1971), *Inelastic Behavior of Steel Beam-to-Column Subassemblages*, Report No. EERC-71/7, Earthquake Engineering Research Center, University of California, Berkeley, CA.

Krawinkler, H. (1978), "Shear in Beam-Column Joints in Seismic Design of Steel Frames," *Engineering Journal*, AISC, Vol. 15, No. 3, pp. 82–91.

Lee, K.-H., Stojadinovic, B., Goel, S.C., Margarian, A. G., Choi, J., Wongkaew, A., Reyher, B.P., and Lee, D. (2000), "Parametric Tests on Unreinforced Connections," Report No. SAC/BD-00/01, SAC Joint Venture, Sacramento, CA.

Lee, D., Cotton, S., Dexter, R.J., Hajjar, J.F., Ye, Y., and Ojard, S. D. (2002), *Column Stiffener Detailing and Panel Zone Behavior of Steel Moment Frame Connections*, Report No. ST-01-3.2, Department of Civil Engineering, University of Minnesota, Minneapolis, MN.

Lee, D., Cotton, S.C., Hajjar, J.F., Dexter, R.J., and Ye, Y. (2005), "Cyclic Behavior of Steel Moment-Resisting Connections Reinforced by Alternative Column Stiffener Details. I. Connection Performance and Continuity Plate Detailing," *Engineering Journal*, AISC, Vol. 42, No. 4.

Leon, R.T. (1983), *The Influence of Floor Members on the Behavior of Reinforced Concrete Beam-Column Joints Subjected to Severe Cyclic Loading,* Ph.D. Dissertation, Department of Civil Engineering, University of Texas, Austin, TX.

Liew, J.Y.R. and Chen W.F. (1995), "Analysis and Design of Steel Frames Considering Panel Joint Deformations," *Journal of Structural Engineering,* ASCE, Vol. 121, No. 10, pp. 1531–1539.

Mao, C., Ricles, J.M., Lu, L., and Fisher, J.W. (2001), "Effect of Local Details on Ductility of Welded Moment Connections," *Journal of Structural Engineering,* ASCE, Vol. 127, No. 9, pp. 1036–1044.

Popov, E.P., Amin, N.R., Louie, J.J.C., and Stephen, R. M. (1986), "Cyclic Behavior of Large Beam-Column Assemblies," *Engineering Journal*, AISC, Vol. 23, No. 1, pp. 9–23.

Prochnow, S.D., Dexter, R.J., Hajjar, J.F., Ye, Y., and Cotton, S. C. (2000), *Local Flange Bending and Local Web Yielding Limit States in Steel Moment-Resisting Connections*, Report No. ST-00-4, Department of Civil Engineering, University of Minnesota, Minneapolis, MN.

Ricles, J. M., Mao, C., Kaufmann, E.J., Lu, L.-W., and Fisher, J.W. (2000), "Development and Evaluation of Improved Details for Ductile Welded Unreinforced Flange Connections," Report No. SAC/BD-00/24, SAC Joint Venture, Sacramento, CA.

Ricles, J.M., Mao, C., Lu, L., and Fisher, J.W. (2002), "Inelastic Cyclic Testing of Welded Unreinforced Moment Connections," *Journal of Structural Engineering,* ASCE, Vol. 128, No. 4, pp. 429–440.

Roeder, C.W. and Foutch, D.A. (1996), "Experimental Results for Seismic Resistant Steel Moment Frame Connections," *Journal of Structural Engineering*, ASCE, Vol. 122, No. 6, pp. 581–588.

Roeder, C.W. (2002), "General Issues Influencing Connection Performance," *Journal of Structural Engineering*, ASCE, Vol. 128, No. 4, pp. 420–428.

SAC (1997), *Protocol for Fabrication, Inspection, Testing, and Documentation of Beam-Column Connection Tests and Other Experimental Specimens*, Report No. SAC/BD-97/02, SAC Joint Venture, Sacramento, CA.

Schneider, S.P. and Amidi, A. (1998), "Seismic Behavior of Steel Frames with Deformable Panel Zones," *Journal of Structural Engineering*, ASCE, Vol. 124, No. 1, pp. 35–42.

Tide, R.H.R. (2000), "Evaluation of Steel Properties and Cracking in k–area of W Shapes," *Engineering Structures*, Vol. 22, No. 2, pp. 128–134.

Tsai, K.C., Wu, S., and Popov, E.P. (1995), "Experimental Performance of Seismic Steel Beam-Column Moment Joints," *Journal of Structural Engineering,* ASCE, Vol. 121, No. 6, pp. 925–931.

UBC (1991), *Uniform Building Code*. International Conference of Building Officials, Whittier, CA.

Wongkaew, A., Goel, S.C., and Stojadinovic, B. (2001), *Development of Improved Details for Unreinforced Welded Steel Moment Connections,* Report No. UMCEE 01-20, Department of Civil and Environmental Engineering, University of Michigan, Ann Arbor, MI.

Ye, Y., Hajjar, J.F., Dexter, R.D., Prochnow, S.C., and Cotton, S.C. (2000), *Nonlinear Analysis of Continuity Plate and Doubler Plate Details in Steel Moment Frame Connections*, Report No. ST-00-3, Department of Civil Engineering, University of Minnesota, Minneapolis, MN.